



**SPE 142211-PP**

## **Recent Advances in Pore Pressure Prediction In Complex Geologic Environments**

Alan R. Huffman<sup>1</sup>, Jeffrey Meyer<sup>1</sup>, Robert Gruenwald<sup>2</sup>, Javier Buitrago<sup>2</sup>, Jaime Suarez<sup>2</sup>, Carlos Diaz<sup>2</sup>, Jose Maria Munoz<sup>2</sup>, Jack Dessay<sup>2</sup> (1) Fusion Petroleum Technologies Inc., (2) Repsol Murzuq S.A.

Copyright 2011, Society of Petroleum Engineers

This paper was prepared for presentation at the SPE Middle East Oil and Gas Show and Conference held in Manama, Bahrain, 20–23 March 2011.

This paper was selected for presentation by an SPE program committee following review of information contained in an abstract submitted by the author(s). Contents of the paper have not been reviewed by the Society of Petroleum Engineers and are subject to correction by the author(s). The material does not necessarily reflect any position of the Society of Petroleum Engineers, its officers, or members. Electronic reproduction, distribution, or storage of any part of this paper without the written consent of the Society of Petroleum Engineers is prohibited. Permission to reproduce in print is restricted to an abstract of not more than 300 words; illustrations may not be copied. The abstract must contain conspicuous acknowledgment of SPE copyright.

### **Abstract**

In recent years, methods have been developed to enable robust pressure prediction in the presence of multiple pressure mechanisms including undercompaction, unloading processes (secondary pressure mechanisms) and at great depth, the onset of secondary chemical compaction. These models utilize geological and geophysical information to constrain the calibration models and the depths at which they must be applied to develop a multi-layer pressure calibration model that will accurately predict pressures for prospect-level analysis and pre-drill prediction. These models are then integrated with the velocity field and the geological and geophysical information to predict pore pressures and fracture pressures at greater depths than have been previously feasible. This methodology has been tested in multiple basins and has been proven to be effective in helping drilling engineers improve well performance through more effective mud and casing program designs that significantly reduces well costs and rig time.

Recent application of elastic and acoustic inversion in complex carbonate environments have also proven effective in predicting pressures in environments where the shales can be separated from the carbonates. The approach requires that the inverted data be separated into the shale and carbonate velocity trends to allow the shales to be used for effective stress prediction while the complete velocity field is used for time-depth conversion. These studies have revealed that pore pressure prediction from mixed lithology (carbonate and shale) environments is feasible using advanced inversion methods. Successful pressure prediction in this type of geology requires seismic data that is of sufficient quality to enable a robust acoustic and/or elastic inversion to be performed that can separate the shale velocities for effective stress calculation, and perform time-depth conversion from the complete velocity field. As the amount of shale present in the geologic section becomes smaller, the ability to predict pressures decreases. The presence of marls also presents a problem because the carbonate material within the shale suppresses the sensitivity of the shale velocity to pore pressure.

### **Introduction**

#### **Basic Approach To Pore Pressure Prediction**

Pressure prediction is typically performed using time-migrated gathers along with well logs and borehole geophysical data from local well control. The method requires detailed velocity analysis on the seismic gathers, some conditioning of the well data, followed by calibration of the seismic with the well data and prediction of fluid pressures on whatever grid was picked on the seismic data. The final velocity picks from the seismic data are calibrated using well control, and a velocity-effective stress transform is determined that honors the well and seismic data at the control well locations. The overburden for the prediction area is calculated by integrating the density log data to obtain a vertical stress versus depth relationship referenced to the mudline or land surface. This equation usually takes the form of

$$\text{Vertical Stress} = a \cdot Z^b$$

where Z is depth, a is a coefficient and b is an exponent.

For this study, a Bowers-type relationship was used to create calibrations for velocity-effective stress. The Bowers equation is a power law relationship between velocity and effective stress that has been proven to be very effective worldwide for interpreting stress and predicting fluid pressure. The basic equation is of the form;

$$V = V_0 + A \cdot \sigma^B$$

where V is the velocity,  $\sigma$  is the effective stress, A is a coefficient and B is an exponent.

The Vertical Stress and Effective Stress are then combined to calculate the pore pressure using Terzhagi's basic relationship:

$$\text{Vertical Stress} = \text{Fluid Pressure} + \text{Effective Stress.}$$

The last item to be calculated is the fracture pressure and fracture pressure gradient. The fracture pressure is usually determined with offset well calibration using a constant percentage of overburden, or using a Matthews and Kelly approach where the fracture pressure is defined as

$$P_f = P_p + K \cdot (OB - P_p)$$

Where  $P_f$  is the fracture pressure, K is the stress ratio,  $P_p$  is the fluid pressure and OB is the overburden (vertical stress). For this study, a Matthews and Kelly approach was employed.

### Prediction Methodology

Geopressure prediction starts with quality control of the existing well data, seismic gathers and velocity data. The initial seismic gathers are conditioned using a proprietary data conditioning work flow. Dense velocity analysis is then performed on the 3D data around the proposed drill location, and these velocity picks are used as the input to residual velocity analysis. Residual velocity analysis using an AVO phase-mismatch methodology is performed on the seismic data using a spatial smoothing of 33x33 CDP's and a temporal smoothing of 480 milliseconds to stabilize the variations in the velocities without distorting the variations across faults and other primary structures.

Because the residual velocities don't have the resolution needed to highlight the velocities of the thin layers of shale and carbonates observed in certain geologic environments, a proprietary thin-bed resolution inversion procedure was used to generate a high resolution model using the residual velocities as the low-frequency constraint and the reflectivity data from the thin-bed inversion for the high-frequency component of the inversion. The inversion result is then used to separate the shale interval velocities over the prospect, and the shale velocity trends are used to generate the final velocity cubes for the shale prediction. The shale trend is used for the effective stress calculation, and the original inverted velocities are used for depth conversion. Figures 1 and 2 show the original residual velocities and the final inverted velocities. Figure 3 shows the inverted trace at a proposed well location along with the shale velocity trend extracted from the inversion.

The fluid pressure prediction is developed by generating vertical stress and seismic velocity/effective stress models from control wells. Pressure data including mud weight, RFT, MDT and LOT data are employed in the calibration procedure to estimate overburden, pore pressure and fracture pressure.

Density logs curve from a control well are integrated to estimate the vertical stress (Figure 4). The red points in the left hand track indicate a representation of the density data. The points in the right hand track indicate the calculated vertical stress (overburden) from this density model. The red curve indicates a mathematical model of the calculated vertical stress:

$$\text{Vertical Stress} = \text{Overburden} = .0019832 \cdot d^{1.0638}$$

where stress is in kpsi and depth (d) is in meters below mudline.

This mathematical model is applied at all locations throughout the velocity volume. In regions where the depth to the top of undercompaction varies spatially, or the extent of undercompaction varies, the use of a single vertical stress function can lead to over/under-estimation of the vertical stress. The vertical stress curve defined in Figure 4 employs a density log with only minor indications of density reversal. The vertical stress will be slightly lower if severe density reversals are present within the study area. Alternatively, if higher densities are present in the survey area, then the model will underestimate the vertical stress. The overburden model is calibrated to the 'high-side' of the data to ensure that vertical stress is not underestimated.

The fluid pressure measurements or mud weights for a well may be combined with the overburden curves to calculate effective stress values as a function of depth. This procedure underestimates the effective stress if the mud weight is greater than the fluid pressure. The mud weight profiles from two control wells in the study area indicate gradually increasing fluid pressure beginning at about 500 meters below the mudline. The MDT and DST data from these wells suggest a hydrostatic fluid pressure profile to at least 2500 meters.

The mud weight curve for the calibration wells can be combined with the overburden model and the velocity data to calculate an effective stress for each mud weight/depth pair (Figure 5). The same process can be applied to the MDT and DST data. When the fluid pressure approximates the mud weight, this approach provides a good interpretation of the fluid pressure/effective stress relationship. When mud weight exceeds the fluid pressure, the most common situation, the mud weight approach tends to overestimate fluid pressure. The data in Figure 5 display considerable scatter. A hybrid interpretation (red curve) was created that honors the minimum fluid pressure model at low effective stress and honors the maximum fluid pressure model at high effective stress.

### **Pre-Drill Prediction**

The calibrations for overburden, pore pressure and fracture pressure are utilized to predict conditions at the original proposed location (Figure 6). The final pore pressure gradient for the proposed well location (blue curve) is relatively stable and smoothly varying with depth. The fracture pressure (orange curve) is also well behaved. The overall pressure environment is relatively benign in the shallow section and then increases steadily below about 3,500 meters to a maximum of about 15.5 PPG at 4,600 meters.

The predicted pore pressure was used to generate a proposed mud weight profile (green curve) that should be sufficient to maintain a slightly overbalanced condition for the entire length of the well bore. This proposed mud weight profile is designed to manage the shale pressures, and also to address potential reservoir pressures in the two target horizons that were modeled. Centroid models for two target reservoirs require only a modest increase in mud weight to manage potential pressure kicks in each of the target zones. The recommended mud program is sufficiently high to manage this reservoir pressure. The predicted mud weight at the TD of the proposed location does not require mud weight greater than about 16 PPG.

Following the initial prediction, a decision was made to move the well location which required an update to the proposed model. Figures 7a and 7b show the comparison of the original prediction location and the revised location. The deep pressure ramp exists at both locations, but the shallow pressure ramp from 2250 to 3500 meters shows a significant difference in the predicted pressure.

### **Well Monitoring Results**

The well was monitored during drilling using conventional data types (mud weight, ROP, gas, etc) along with onsite pressure monitoring while drilling. Figure 8 shows the original prediction with the monitoring data including the actual mud weights (blue squares), pressure while drilling data (red dots), MDT pressures (green diamonds) and Leak Off Tests (black diamonds). The initial prediction in the section from 2250 to 3500 was confirmed to be too high because of the presence of open fractures which caused total losses of drilling fluids. The losses required that the mud weight be reduced back to hydrostatic to resolve the issue. Once the open fractures healed at the top of the predicted pressure ramp, the actual pressures began tracking the prediction very nicely. The reservoirs with permeability confirmed that the prediction for the deep section was robust and confirmed the validity of the inversion approach in this complex environment. Application of the same method using the shale trend from the Vertical Seismic Profile (VSP) data confirmed the same result (Figure 9).

## **Conclusions**

The prediction of pore pressure and fracture pressure using shale velocities from an inversion-based separation of shale from other lithologies has been proven to be effective in complex geologic environments. The method requires seismic data of sufficient quality to allow the separation to be performed, and sufficient offset well data to calibrate the shale effective stress trend for the proposed location. The application of the method to 3D seismic data provides the added benefit of spatial variations in the pressure regime that can be used to predict centroid pressures in reservoirs in 3D along with fault seal and other critical parameters for prospect risking.

## **Acknowledgements**

The authors wish to acknowledge the support of Repsol Murzuq and Fusion Petroleum Technologies Inc. which approved the release of data and information for this paper.

Figures

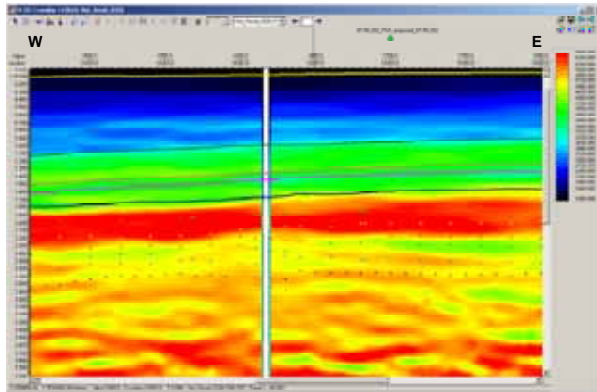


Figure 1: Residual velocities over the prospect area

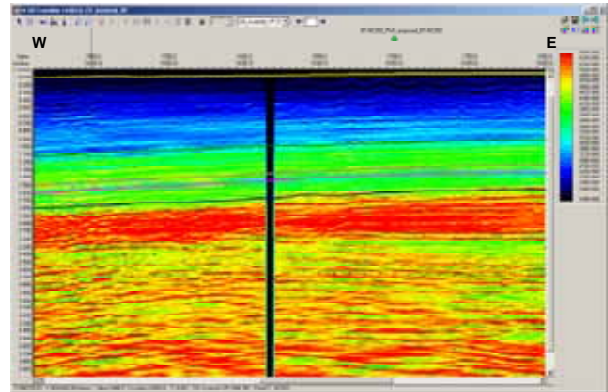


Figure 2: Inverted velocities over the prospect area

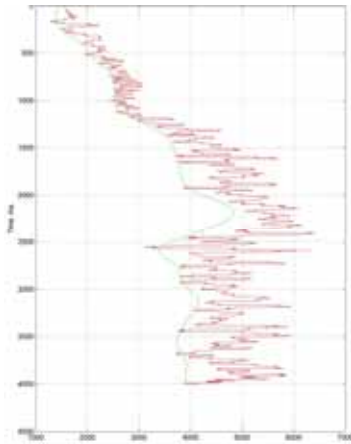


Figure 3: Shale (green) and inversion (red) velocities at the proposed location.

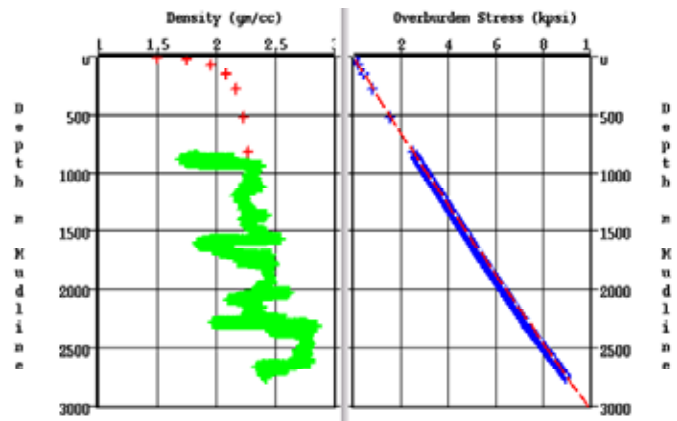


Figure 4: Estimation of overburden stress from density log data

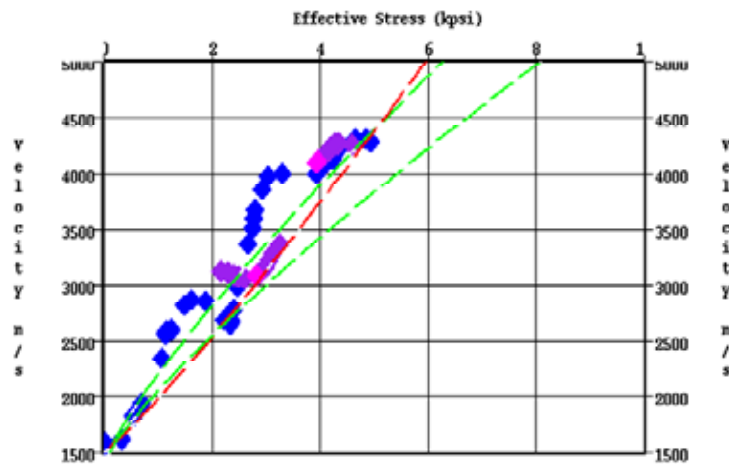


Figure 5: Effective stress diagram showing the maximum and minimum stress curves (green) and final hybrid stress calibration (red curve).

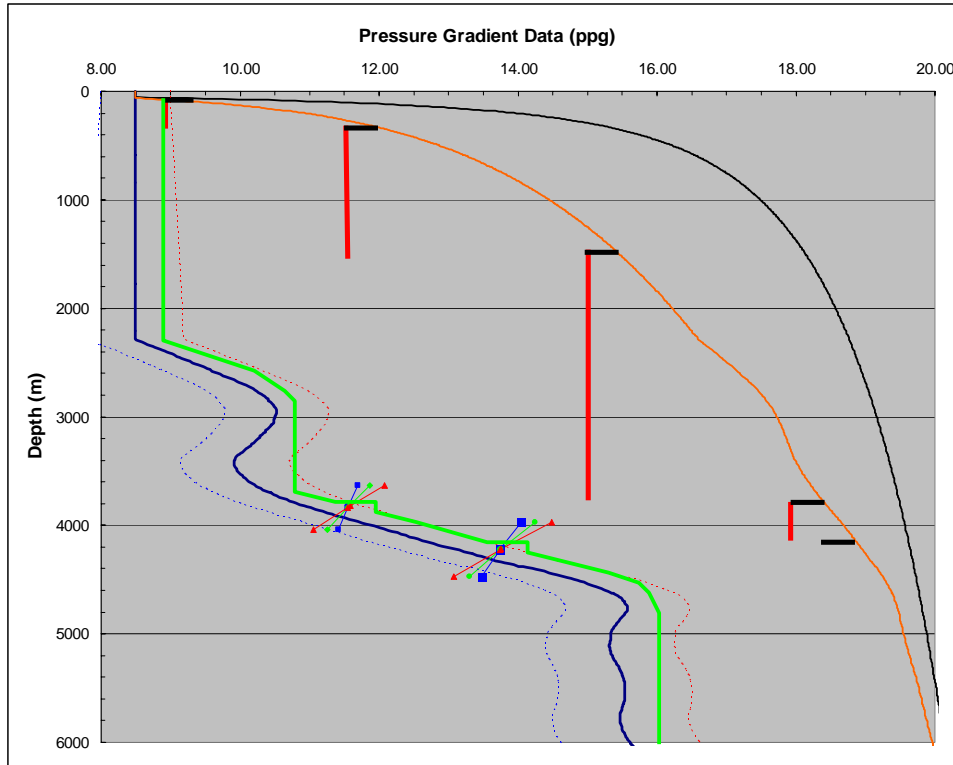


Figure 6: Pre-drill prediction at original well location showing shale pressure (blue), fracture pressure (orange), overburden (black), and proposed mud weight (green). Also shown are proposed leak off depths (short black lines) and casing runs (red lines).

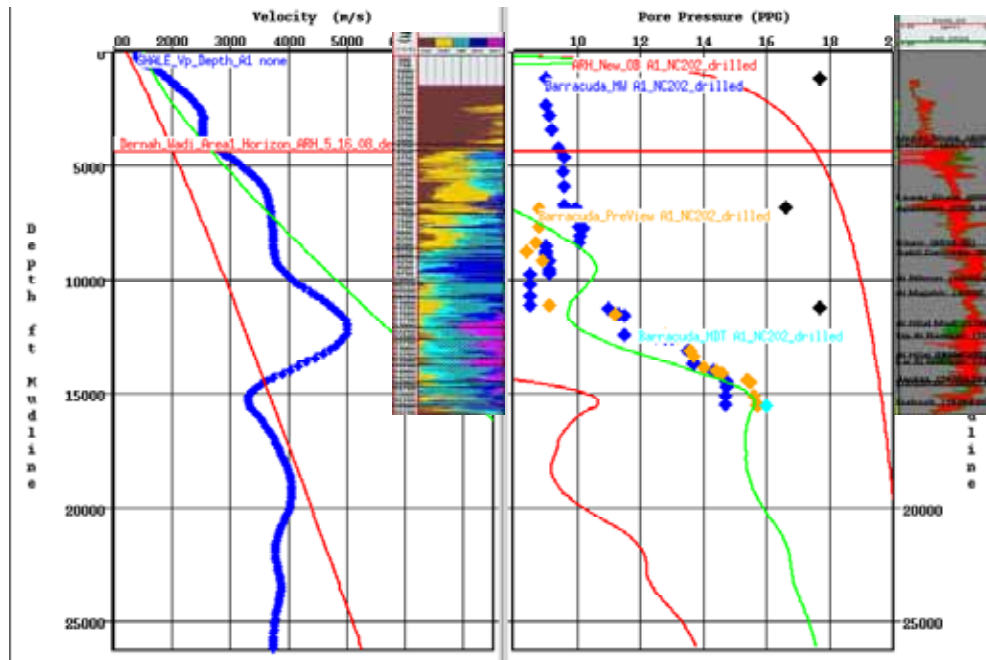


Figure 7a: Predrill prediction at original drilling location showing actual mud weights (blue diamonds), pressure while drilling data (orange diamonds), MDT data (cyan diamonds) and Leak off tests (black diamonds).

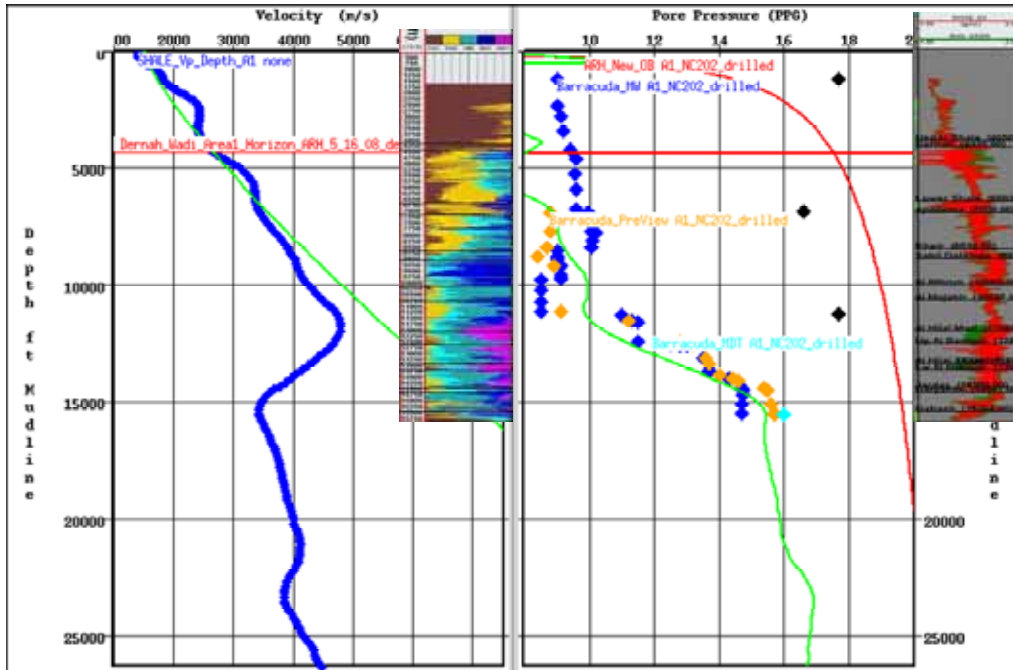


Figure 7b: Post-drill pressure data at final well location showing actual mud weights (blue diamonds), pressure while drilling data (orange diamonds), MDT data (cyan diamonds) and Leak off tests (black diamonds).

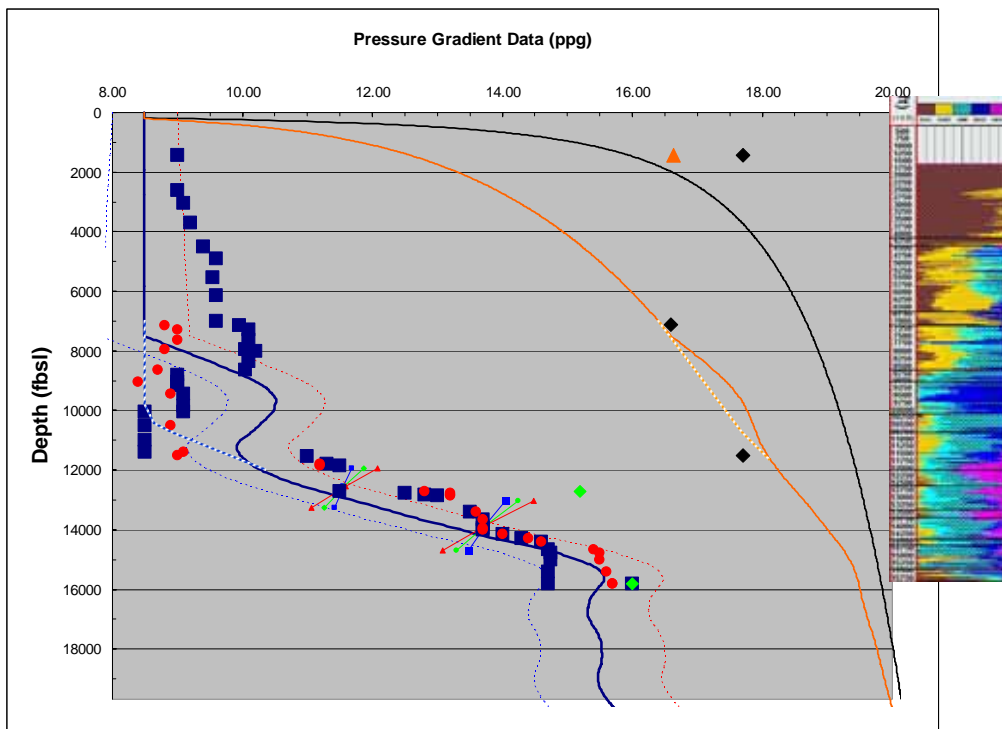


Figure 8: Post-drill pressure data at final well location showing actual mud weights (blue diamonds), pressure while drilling data (orange diamonds), MDT data (cyan diamonds) and Leak off tests (black diamonds).

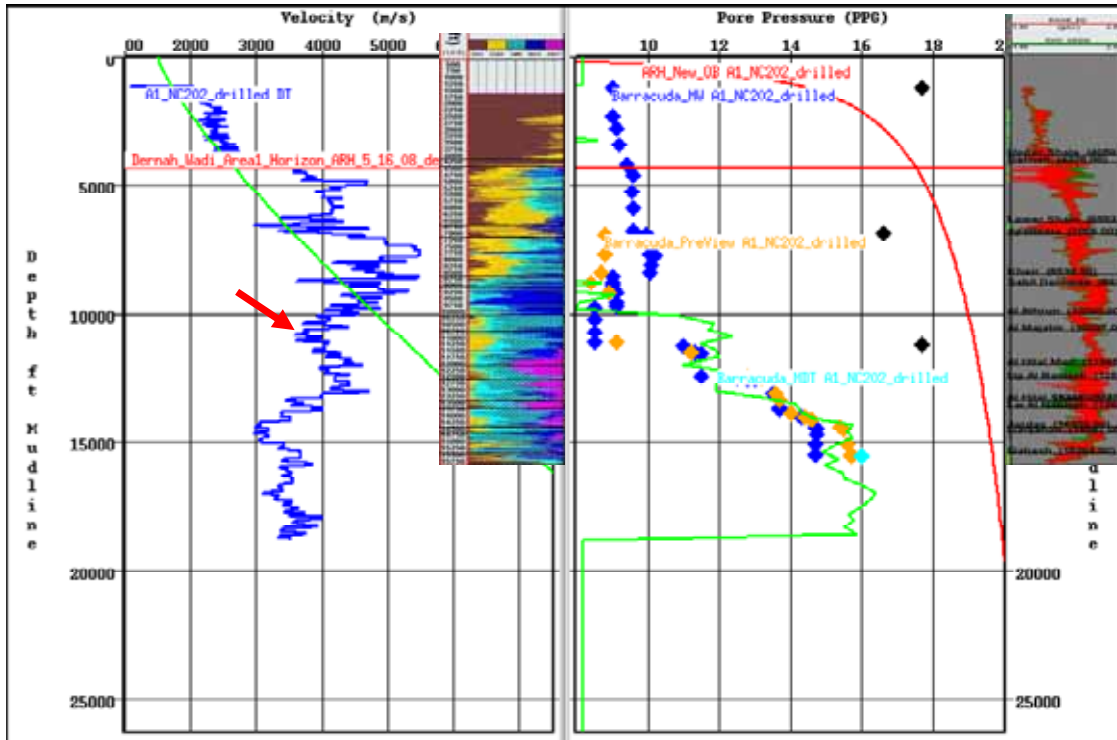


Figure 9: VSP-based prediction of pressures at the final well location showing showing actual mud weights (blue diamonds), pressure while drilling data (orange diamonds), MDT data (cyan diamonds) and Leak off tests (black diamonds).